The consequences of high injected carrier densities on carrier localisation and efficiency droop in InGaN/GaN quantum well structures

S. Hammersley[1], D. Watson-Parris[1], P. Dawson[1], M. J. Godfrey[1], T. J. Badcock[1], M. J. Kappers[2], C. McAleese[2], R. A. Oliver[2] and C. J. Humphreys[2]

1. *School of Physics and Astronomy, Photon Science Institute, Alan Turing Building, University of Manchester, Manchester, M13 9PL, United Kingdom*

2. *Department of Materials Science and Metallurgy, University of Cambridge Pembroke Street, Cambridge, CB2 3QZ, United Kingdom*

There is a great deal of interest in the underlying causes of efficiency droop in InGaN/GaN quantum well light emitting diodes, with several physical mechanisms being put forward to explain the phenomenon. In this paper we report on the observation of a reduction in the localisation induced S-shape temperature dependence of the peak photoluminescence energy with increasing excitation power density. This S-shape dependence is a key fingerprint of carrier localisation. Over the range of excitation power density where the depth of the S shape is reduced we also observe a reduction in the integrated photoluminescence intensity per unit excitation power, i.e. efficiency droop. Hence the onset of efficiency droop occurs at the same carrier density as the onset of carrier delocalisation. We correlate these experimental results with the predictions of a theoretical model of the effects of carrier localisation due to local variations in the concentration of the randomly distributed In atoms on the optical properties of InGaN/GaN quantum wells. On the basis of this comparison of theory with experiment we attribute the reduction in the S-shape temperature dependence to the saturation of the available localised states. We propose that this saturation of the localised states is a contributory factor to efficiency droop whereby non localised carriers recombine non-radiatively.

*Electronic mail:philip.dawson@manchester.ac.uk

Introduction

Light emitting diodes (LEDs) that utilise InGaN/GaN quantum wells as the active region are already having significant impact in high brightness displays and many other applications. One of the most important problems that is preventing further exploitation of InGaN based LEDs in applications that require very high light output such as solid state lighting is the so-called efficiency droop[1,2]. At high injection currents, of the order 10 A cm^{-2}, the room temperature external quantum efficiency of LEDs drops significantly. There is currently much debate as to the mechanism(s) responsible for efficiency droop. The main mechanisms proposed include hole injection efficiency[3,4] Auger recombination[5] and carrier escape[6], it should be noted in particular in the context of this paper that the conclusions drawn in the work of Jinqiao et al[3] were based on the observation of no efficiency droop in photoluminescence (PL) measurements. This disagrees with our results (see later). Concerning Auger recombination, this proposal was initially was based on analysis of high current density efficiency[5] and photoluminescence time decay measurements[7] using the so-called A, B, C model. More recently using resonant optical excitation and measurements of the photocurrent at high forward bias Schubert et al[6] proposed that carrier escape played a role in efficiency droop.

Carrier localisation is widely believed [8,9,10,11,12,13] to be responsible for the high room temperature recombination efficiency of InGaN/GaN quantum well structures; however, this localisation was believed to occur at gross In-rich clusters in the InGaN quantum wells. Smeeton et al[14] showed that such clusters were an artefact caused by electron beam damage in electron microscopy and hence could not be responsible for carrier localisation. Galtrey et al[15] then showed that InGaN was a random alloy with

In atoms distributed at random on Ga sites according to a binomial distribution. Graham et al[16] showed that carriers could be localised at monolayer interface steps in the quantum wells, as suggested by electron microscopy, and such quantum well thickness fluctuations were confirmed by atom probe tomography[17]. The random fluctuations of In in InGaN QWs and the thickness fluctuations of the quantum wells localise the carriers, thus preventing them from diffusing to defects and hence resulting in a high efficiency of light emission[18]. Hader et al[19] suggested that efficiency droop might be due to density activated defect recombination. At low current densities the carriers are localised at local in-plane potential minima, with increasing current density a significant fraction of the carrier population might not be localised and might be free to recombine non-radiatively at defects. The conclusions reached by Hader et al[19] are similar to those of Wang et al[20] although the latter attributed efficiency droop to a combination of carrier delocalisation and carrier leakage.

To further investigate the droop problem we have performed a series of photoluminescence measurements over a range of excitation power densities and temperatures to simultaneously investigate the photoluminescence efficiency and carrier localisation in InGaN/GaN quantum wells. Furthermore, we have compared our results with a theoretical model of carrier localisation that considers the effects of the random distribution of In atoms in InGaN.

Experimental Details

The InGaN/GaN 5-period quantum well structure studied in this work was grown on a 5 μm thick GaN buffer layer, the buffer layer was grown in a Thomas Swan 6x2" metalorganic vapour-phase epitaxy reactor using trimethyl gallium (TMG), silane

(SiH_4) and ammonia (NH_3) as precursors, with hydrogen as the carrier gas. The GaN buffer layer was deposited at 1020 °C on a (0001) sapphire substrate with a 0.25±0.10° miscut towards (11-20) following the growth of a low-temperature (530 °C) GaN nucleation layer[21]. The threading dislocation density of the GaN buffer layer was ~3×10^8 cm^{-2} as measured by an atomic force microscopy assessment of modified surfaces[22]. The quantum wells were grown using a two-temperature method where the temperature was 715 and 860 °C for the growth of wells and barriers, respectively, and no growth took place during the temperature ramps. The metal precursors used were trimethyl gallium (TMG) and trimethyl indium (TMI) and the carrier gas was nitrogen at a constant pressure of 300 Torr. The InGaN quantum wells were grown in 197s using a flow of 4.4 μmol/min of TMG and 14.5 μmol/min of TMI, while the GaN barrier growth time was 37s using a TMG flow of 67 μmol/min. The ammonia flow was constant at 446 mmol/min throughout the MQW growth.   High-resolution X-ray measurements[23] showed that the 5-period QW structure consisted of 1.9 nm wide InGaN wells with an average indium fraction of 0.13 separated by 6.3 nm wide GaN barriers.

For the optical measurements the sample was mounted on the cold finger of a closed cycle helium cryostat at temperatures between 10K and 300K. The chopped output from a frequency doubled mode-locked Ti:sapphire laser was used to excite the sample with a photon energy greater than the GaN barrier band gap at average power densities between 1 W cm^{-2} and 10,000 W cm^{-2}. The excitation light was focussed onto the sample surface using a microscope objective and the spot size determined by the standard technique using a stepper motor driven knife edge. To avoid the effects of interference[16] on the PL spectra produced by the etalon defined by the GaN/air interface and the GaN/sapphire interface the sample was inclined at Brewster's angle

to the collection optics and the light passed through a linear polariser. In this configuration only that polarisation of light that is not reflected at the GaN/air interface is collected. The photoluminescence emission was focussed onto the slits of a 0.85m spectrometer and the light detected by a GaAs photomultiplier tube. The time-averaged signal from the photomultiplier was then processed using standard lock-in techniques.

Experimental Results

To further investigate the report by Jinqiao et al[3] that efficiency droop could not be observed in optical excitation experiments we carried out a series of power density dependent PL measurements. Initially we present the data taken at a temperature of 10K. The PL intensity is shown in Figure 1 over the range of excitation power densities 1 to 10,000 W cm^{-2}. In the low excitation power density range 1 to 100 W cm^{-2} we found that the integrated PL intensity per unit excitation power remained constant. When the excitation power density was greater than 30 W cm^{-2} the integrated PL intensity per unit excitation power began to fall until at power densities approaching 10,000 Wcm^{-2} it had fallen by almost 80%. We attribute the fall in integrated PL intensity per unit excitation power at power densities greater than 30 Wcm^{-2} to efficiency droop. We note that similar data were observed up to room temperature, so the drop in efficiency is not determined by the measurement temperature.

As most of the measurements of efficiency droop have been made on LEDs then it is important that we try to relate our optical measurements to the current densities at which LED droop is observed. The factors in doing this estimate that are least certain are the carrier collection efficiency and the carrier lifetime. Based on the fact that we

did not observe any significant PL from other recombination channel other than intrinsic recombination from the quantum wells leads us to assume that the quantum well carrier collection efficiency is close to 100% and that the carriers are distributed equally between the wells. The lifetime factor is more problematic in that PL decay measurements across the InGaN/GaN quantum well PL line shape have revealed that the decay curves are non exponential and that the recombination lifetimes as defined by the time taken for the intensity of the light to fall by 1/e vary with detection energy[11]. To overcome these difficulties in calculating equivalent sheet carrier densities we use the time for the PL measured at the peak of the spectrum to decay by a factor of 1/e. Using a value of 6.2 ns results in an estimated equivalent CW current density of 30A cm^{-2} for which the recombination efficiency was a maximum. Despite the limitations of the estimate of the CW current density this figure compares well with reported values of the onset of droop in LEDs[24, 25, 26, 27,28,29,30]. The equivalence of electrical and optical measurements of the droop is supported by the recent work of Laubsch et al[30].

To further investigate the mechanism responsible for efficiency droop we studied the temperature dependent PL spectra and integrated intensity as a function of excitation power density. Figure 2 shows the changes of the peak position of the PL spectrum with increasing temperature at excitation power densities of 1.2 and 7.2 x 10^3 Wcm^{-2}; it should be noted that the temperature dependence of the InGaN bandgap has been removed from the plotted values of the change in peak position. At low excitation power densities the temperature dependence of the peak energy of the recombination from InGaN/GaN quantum wells exhibits the well known S-shape. This dependence has been widely studied and has been attributed[31, 32, 33, 34] to the thermally activated rearrangement of carriers within the distribution of localised states in the InGaN/GaN

quantum well. Near 0K the carriers are randomly distributed amongst the localising centres and they recombine with a correspondingly broad range of energies. Between 25 and 75K the carriers are able to scatter into low energy states and remain there until recombination, leading to a blue shift of the peak of the recombination spectrum. At temperatures above ~ 100K, as the carriers gain enough energy so that they can be distributed across the range of localised states. We note in particular that even up to the highest temperature measured that the carriers remain distributed amongst the localised states as has been discussed elsewhere [11, 35, 36, 37, 38].

The data in figure 2 reflects this behaviour but the classical S shape is not evident since we have removed the temperature dependence of the InGaN bandgap from the data. When the power density is increased the depth of the minimum is greatly reduced and for the excitation power density of 7.2×10^3 Wcm^{-2} it is almost absent, as shown in Fig. 2. To quantify this effect we compared the results of the change in peak position versus temperature experiment with the following equation[31]:

$$E = E(0) - \frac{\sigma^2}{kT} \qquad (1)$$

Where E is the energy of the peak of the PL spectrum, E (0) is the energy of PL peak at 10K and σ is representative of the average energy of localisation[31]. In the original work by Eliseev et al[31] the full expression for the change in E contains separate σ terms for the distribution of localised electron and hole states. Hence, in the expression above σ represents the distribution of whichever carrier type that determines the S shape behaviour.

Figure 3 shows a plot of the extracted values of σ versus excitation power density. At low excitation power densities, below 10W cm^{-2} σ remains constant at ~10meV, but as the excitation power density increases σ steadily decreases until at the highest excitation power density σ is reduced to almost zero. We initially ascribe the

apparent reduction in σ to the effects of the saturation of the localised states. When all the states are filled there can be no thermally induced rearrangement of the carriers between available states and thus σ goes to zero. This explanation is confirmed by the theoretical analysis discussed in detail later. To shed further light on this we compare our data with the predictions of a theoretical model of the effects of the microstructure on the optical properties of InGaN quantum wells.

Theoretical Model

In this section we outline the principles of the theoretical model we have used to enable a through interpretation of our experimental data, the details of the model have been described elsewhere[39,40]. We ascribe carrier localisation to the effects of well width fluctuations *and* random variations in the concentration of In atoms. Atom probe tomography[41] measurements have revealed that the active regions of InGaN/GaN quantum wells grown with a single temperature for both wells and barriers contain InGaN which is a purely random alloy with no evidence of In clustering, and that the interface that is grown first (the lower interface) is smooth and the upper interface is rougher. The quantum wells reported on here were grown using so-called quasi two temperature growth which can lead to variations of the average In content on a length scale of ~100 nm. As discussed in detail later such a length scale is much greater than those which determine the optical properties reported on here and thus we will treat the InGaN as a random alloy.

By solving Schrödinger's equation for quantum wells where the energy landscape reflects the effects of random alloy fluctuations and well width fluctuations we were able to calculate the localisation energies of electrons and holes. The overall picture that emerges from this treatment, neglecting any Coulomb interaction between

electrons and holes, is that at low temperature holes are strongly localised by the statistical fluctuations in the In concentration, and electrons are more weakly localised by a combination of In fluctuations and variations in quantum well width. The calculated energies of the localised electrons and holes enables a comparison to be made between the theoretically predicted photoluminescence spectrum and the zero phonon PL spectrum measured at low temperature. A comparison of the results of the theoretical model and the measured low temperature PL spectrum of a 3.3 nm thick $In_{0.25}Ga_{0.75}N$/GaN single quantum well is shown in reference 40. The theoretical model predicts a FWHM of the spectrum of 69 meV, which is similar to the measured value 63 meV. The major contributory factor to the line width is due to variations in hole localisation. Adding in the effects of well width fluctuations had very little effect on the predicted line shape. Thus it was concluded that the major contribution to the low temperature recombination line width from InGaN/GaN quantum wells is the variation in hole confinement and the local In environment at the different localisation sites.

We now discuss an extension of this localised state model that allows us to model the temperature dependence of the PL spectrum as well as the effects of varying the excited carrier density. To do this we introduce the effects of phonon scattering on the distributions of the excited electron and hole populations making the following assumptions: Firstly, we only consider the effects of acoustic phonons as the energy of optical phonons are so large that they can be neglected when considering scattering and diffusion between localised states. Secondly we assume that the interaction of the acoustic phonons with the carriers is sufficiently weak that it can be considered as a perturbation to the zero temperature calculations. Thirdly we ignore any Coulomb interaction between the excited carriers. The rates for scattering via the interaction

with acoustic phonons were calculated using the carrier wave functions, and the resulting master equation for the distribution of the carriers was solved by a Monte Carlo method[42].

In Figure 4 we show the predicted change in peak position as a function of temperature, not including any temperature dependence of the InGaN bandgap, for a 3.0 nm thick $In_{0.12}Ga_{0.88}N$/GaN single quantum well. The underlying cause of this behaviour is the thermally driven redistribution of carriers amongst the localised states. More specifically the redistribution of holes is responsible for the predicted change in the peak position of the recombination spectrum. This is apparent if we extend the results of our model to show how the diffusion energy of both electrons and holes changes as a function of temperature. We define the electron/hole diffusion energy as the average change in energy of electrons/holes after random occupation of localised states followed by diffusion to a final state where radiative recombination occurs. As we noted previously[40] our model suggests that the localisation energy of holes is much larger than that of electrons. Thus, as shown in figure 5 the change in diffusion energy for holes is much larger than that for electrons and the magnitude of the change for holes is closely matches the predicted change in PL peak position as shown in figure 4. The agreement between the experimental data in figure 2 and the theoretical date in figure 4 is reasonable, with both sets of data exhibiting minima at the same temperature and with the minimum values of σ being 11 ± 2 meV and 11 ± 7 meV for the experimental data and theoretical data respectively.

We now consider the experimentally observed flattening of the S shape at high carrier densities. To enable a direct comparison of the predictions of the theoretical model and the experimental data presented earlier we fit the predicted peak shift above T =

50K to equation (1). Using the extracted values of σ this allows us to compare directly the results of our model with the experimentally determined values of σ.

In figure 6 we show the predicted values of σ along with the occupation fractions of the electron and hole states for different values of the calculated excitation power densities. It can be seen in figure 6(b) that the electron states saturate when the excitation power density is as low as 10W cm^{-2}. As the power density is increased even further the hole states start to saturate and the value of σ decreases. The implication of the data in figure 6 is that the saturation of the electron states has little effect on the parameter that is measured experimentally, i.e. σ. This is in line with our previous conclusion that the form of the PL spectra is determined by the spread in hole localisation energies. So, as we see from figure 6, once the hole state occupation factor starts to saturate then σ begins to change.

The insight our theoretical model brings to the underlying microscopic behaviour responsible for the changes in the spectral behaviour with increasing carrier density now allows us to discuss the reason for the efficiency droop we observed experimentally. Our theoretical model enables us to calculate the diffusion lengths of both the electrons and holes as a function of temperature. We will not discuss these results in detail here but they are comprehensively addressed elsewhere[42]. To summarise these results the model predicts, assuming independent electrons and holes, average diffusion lengths for electrons at low temperature to be ~50nm increasing progressively to ~250nm at room temperature and for holes at low temperature 2nm and increasing to 10nm at room temperature. The parameters that control the magnitudes of these average diffusion lengths which involves localised hopping are the localisation lengths and the density of localised states. The room temperature values for diffusion length of the holes quoted above are less than the

values from room temperature cathodoluminescence measurements[43] on GaN in the vicinity of dislocations of 50nm. More recently time of flight measurements[44] on an $In_{0.26}Ga_{0.74}N/GaN$ multiple quantum well structure have led to a determination of the ambipolar lateral diffusion coefficient to be 0.25 cm^2 s^{-1} at room temperature, in this work it is suggested that the quantum well system in question would have a radiative lifetime of 16ns. This then leads to a diffusion length when only radiative recombination occurs of 600nm.

The small values of diffusion lengths which our model predicts, even at room temperature, would prevent the majority of electrons or holes from recombining at the most likely non radiative centres in InGaN/GaN quantum wells, i.e. dislocations. So even in structures with dislocation densities ($\sim 10^8$ cm^{-2}), as is typical for structures grown on sapphire substrates[45], we would expect, and indeed do observe [46], very high recombination quantum efficiencies. This picture breaks down once the excited population densities are sufficiently high that significant saturation of the electron/hole localised states occurs. In this situation a significant fraction of the excited electrons or holes will be free to diffuse with no great influence from the localisation sites and we may expect much greater diffusion lengths for this subset of the excited carriers. Thus this delocalised fraction of the excited state population can recombine non radiatively (possible at the dislocations) leading to a reduction in the radiative recombination efficiency.

The results, both experimental and theoretical, presented here are in good agreement with this overall model in that at the same carrier densities where we observe a reduction in the S shape dependence of the PL peak position versus temperature we also observe a reduction in the efficiency of recombination, i.e. efficiency droop. A clear suggestion from our theoretical results (see figure 6), is that as the saturation of

the electron localised states occurs at lower power densities than that required to saturate the hole states and the loss of hole localisation governs the temperature dependence of the spectra we might expect droop to occur at a lower excitation power density than that required to bleach the S shape. This is not observed experimentally and may be due to the assumption of independent electrons and holes as well as assumptions made about the calculation of the equivalent excitation power densities.

Summary

In summary, we have performed comparative measurements on an InGaN/GaN multiple quantum well structure of the integrated PL intensity per unit power versus excitation power density and the spectral dependence of the peak energy of recombination as a function of excitation power density. We observed that at the high excitation power densities when a reduction in the photoluminescence intensity per unit power occurred we also measured a reduction in the depth of the S shape temperature dependence of the PL peak energy. We suggest the "bleaching" of the S shape is due to saturation of localised states in the quantum wells which thus leads us on to propose that the reduction in efficiency is a consequence of the localised state saturation in that the delocalised are more able to be transported to non radiative recombination centres.

These conclusions are supported by the results of a theoretical model in which the effects of the random distribution of In atoms in the InGaN quantum wells are considered. The random distribution leads to localised regions of high In concentration that are particularly effective at localising photo-excited carriers. We have shown previously[40] that the spread in localisation energies of holes is much greater than that of electrons so this effect is the dominant contribution to the low

temperature inhomogeneous PL line width. In this paper we have extended this model to include the effects of acoustic phonon scattering leading to a prediction of the PL peak energy shift with increasing temperature that is in reasonable agreement with that measured. The extent of the shift is governed by the thermal redistribution of the carriers whose spread in energy is the dominant contribution to the PL line shape, i.e. the photo-excited holes. The predicted form of the shift is similar to that observed experimentally and furthermore the "bleaching" at increased carrier density is in line with that observed experimentally. At the microscopic level the model also predicts that at the carrier density required for the S shape "bleaching" that both the electron and hole localised states are saturated. This supports our conclusion that localised state saturation plays a role in the reduction in PL efficiency at high excited carrier densities.

Acknowledgements

References

1. H. Morkoc, Handbook of Nitride Semiconductors and Devices (Wiley-VCH, Berlin, 2008), Vol3.

2. J. Xie, X Ni, Q. Fan, R. Shimada, U. Ozgur and H Morkoc, Appl. Phys. Lett. **93**, 121107 (2007).

3. X. Jinqiao, N. Xianfeng, F. Qian, S. Ryoko, O. Umit and M. Hadis, Appl. Phys. Lett. **93**, 121107 (2007).

4. I. A .Pope, P. M. Smowton, P. Blood, J. D. Thompson, M J Kappers and C J Humphreys, Appl. Phys. Lett, **82,** 2755 (2003).

5. N. F. Gardner, G. O. Muller, Y. C. Shen, G. Chen, S. Watanabe, W. Gotz and M. R. Krames, Appl. Phys. Lett. **91**, 243506 (2007).

6. M. Schubert, J. Xu, Qi Dai, F. W. Mont, K. Jong Kyu Kim and E. F. Schubert, Appl. Phys. Lett. **94**, 081114 (2009)

7. Y. C. Shen, G. O. Mueller, S. Watanabe, N. F. Gardner, A. Munkholm and M. R. Krames, Appl. Phys. Lett. **91**, 141101 (2007)

8. S. Chichibu, K. Wada, and S. Nakamura, Appl. Phys. Lett. **71**, 2346 (1997).

9. K. L. Teo, J. S. Coulton, P. Y. Yu, E. R. Weber, M. F. Li, W. Liu, K. Uchida, H. Tokunaga, N. Akutsu and K. Matsumoto, Appl. Phys. Lett. **73**, 1697 (1998).

10. J. Bai, T. Wang, and S. Sakai, J. Appl. Phys. **88**, 4729 (2000).

11. J. A. Davidson, P. Dawson, T. Wang, T. Sugahara, J. W. Orton, and S.Sakai, Semicond. Sci. Technol. **15**, 497 (2000).

12. I. L. Krestnikov, N. N. Ledentsov, A. Hoffman, D. Bimberg, A. V. Sakharov, W. V. Lundin, A. F. Tsatsul'nikov, A. S. Usikov, zh. I. Alferov, Yu. G. Musikhin and D. Gerthsen, Phys. Rev. B **66**, 155310 (2002).

13. H. Schömig, S. Halm, A. Forchel, G. Bacher, J. Off, and F. Scholz, Phys. Rev. Lett. **92**, 106802 (2004).

14. T. M. Smeeton, M. J. Kappers, J. S. Barnard, M. E. Vickers and C. J. Humphreys, Appl. Phys. Lett. **83**, 5419 (2003).

15. M. J. Galtrey, R. A. Oliver, M. J. Kappers, C. J. Humphreys, D. J. Stokes, D. H. Clifton and A. Cerezo, Appl. Phys. Lett. **90**, 061903 (2009).

16. D. M. Graham, A. Soltani-Vala, P. Dawson, M. J. Godfrey, T. M. Smeeton, J. S. Barnard, M. J. Kappers, C. J. Humphreys and E. J. Thrush, J. Appl. Phys. **97**, 103508 (2005).

17. M. J. Galtrey, R. A. Oliver, M. J. Kappers, C. J. Humphreys, P. H. Clifton, D. Larson, D. W. Saxey and A. Cerezo, J. Appl. Phys. **104**, 013524 (2008).

18. C. J. Humphreys, Philos. Mag. **87**, 1971 (2007).

19. J. Hader, J. V. Moloney and S. W. Koch, Appl. Phys. Lett. **96**, 221106 (2010).

20. J. Wang, L. Wang, W. Zhao, Z. Hao and Y. Luo, Appl. Phy. Letts. **97**, 201112 (2010).

21. S. Das Bakshi, J. Sumner, M.J. Kappers, R.A. Oliver, J of Crystal Growth **31**, 232 (2009).

22. R.A. Oliver, M.J. Kappers, J. Sumner, R. Datta, C.J. Humphreys, Journal of Crystal Growth, 289, 506 (2006).

23. M.E. Vickers, M.J. Kappers, T.M. Smeeton, E.J. Thrush, J.S. Barnard, C.J. Humphreys, J. Appl. Phys. **94**, 1565 (2003).

24. A David, Appl. Phys. Letts. **94**, 103504 (2010)

25. A David, Appl. Phys. Letts. **97**, 193508 (2010)

26. J.-R Chen, Appl. Phys. **B 98**, 779 (2010).

27. Yun-Li Li, IEEE J. of Selected Topics in Quantum Electronics **15**, 1128 (2009).

28. K. Ding, Appl. Phys. **B 97**, 465 (2009).

29. M Meneghini, J. Appl. Phys. **106**, 114508 (2009)

30. A Laubsh, IEEE Transactions on Electron Devices **57**, 79 (2010).

31. P. G. Eliseev, P. Perlin, J. Lee, and M. Osinski, Appl. Phys. Letts. **71**, 569 (1997).

32. C. Yong-Hoon, G. H. Gainer, A. J. Fischer, J. J. Song, S. Keller, U. K. Mishra and S. P. Denbars, Appl. Phys. Lett. **73**, 1370 (1998).

33. O. Rubel, M. Galluppi, S. D. Baraovskii, K. Volz, L. Geelhaar, H. Riechert, P. Thoma and W. Stolz, J. Appl. Phys. **98**, 063518 (2005).

34. O. Rubel, S. D. Baraovskii, K. Hantke, W. W. Ruhle, P. Thoma, K. Volz and W. Stolz, Phys Rev. B **73**, 233201 (2006).

35. S. F. Chichibu, H. Marchand, M. S. Minsky, S. Keller, P. T. Fini, J. P. Ibbetson,S. B. Fleischer, J. S. Speck, J. E. Bowers, E. Hu, U. K. Mishra, S. P. DenBaars,T. Deguchi, T. Sota, and S. Nakamura, Applied Physics Letters, **74**, 1460 (1999).

36. E. S. Jeon, V. Kozlov, Y.-K. Song, A. Vertikov, M. Kuball, A. V. Nurmikko, H. Liu, C. Chen, R. S. Kern, C. P. Kuo, and M. G. Craford, Appl. Phys. Letts. **69**, 4194, (1996).

37. S. Chichibu, T. Azuhata, T. Sota, and S. Nakamura, Appl. Phys. Letts. **69**, (1996).

38. J.H. Chen, Z.C. Feng, J.C. Wang, H.L. Tsai, J.R. Yang, A. Parekh, E. Armour, and P. Faniano, J of Crystal Growth, **287**, 354, (2006).

39. D. Watson-Parris, M. J. Godfrey1, R. A. Oliver, P. Dawson, M. J. Galtrey, M. J. Kappers, and C. J. Humphreys, Phys. Status Solidi **C7**, 2255 (2010)

40. D. Watson-Parris, M. J. Godfrey, P. Dawson. R. A. Oliver, M. J. Galtrey, M. J. Kappers, and C. J. Humphreys, Phys. Rev. B **83**, 115321 (2011).

41. M J. Galtrey, R. A. Oliver, M. J. Kappers, C. J. Humphreys, D. J. Stokes, P. H. Clifton and A. Cerezo, Appl. Phys. Letts. **90**, 061903 (2007).

42. Duncan Watson-Parris, PhD thesis, University of Manchester, 2011.

43. T. Sugahara, H. Sat, H. Maosheng, N. Yoshiki, S. Kurai, S. Tottori, K. Yamashita, K. Nishino, L. T. Romano and S. Sakai,, Jpn. J. of Appl. Phys. **37**, L398 (1998).

44. J. Danhof, U. T. Schwarz, A. Kneta and Y. Kawakami, Phys. Rev. B**84**, 035324 (2011).

45. R. Datta, M.J. Kappers, M.E. Vickers, J.S. Barnard, C.J. Humphreys, Superlattices and Microstructures **36**, 393 (2004); R.A. Oliver, M.J. Kappers, J. Sumner, R. Datta, C.J. Humphreys, Journal of Crystal Growth **289**,506 (2006).

46. C. E. Martinez, N. M. Stanton, A. J. Kent, D. M. Graham P. Dawson, M. J. Kappers and C. J. Humphreys, Journal of Applied Physics, **98**, 053509 (2005); D.M. Graham, P. Dawson, M.J. Godfrey, M.J. Kappers, P.M.F.J. Costa, M.E. Vickers, R. Datta, C.J. Humphreys and E.J. Thrush, Physica Status Solidi C **3(6)**, 1970 (2006).

Figure Captions

Figure 1. Integrated photoluminescence intensity per unit power against the incident power density upon the sample.

Figure 2. Measured photoluminescence peak shift with the temperature dependence of the InGaN removed from the data versus temperature for power densities of 1.2 W cm^{-2} and 7.2 kW cm^{-2}.

Figure 3. Extracted values of σ as a function of excitation power density.

Figure 4. Calculated photoluminescence peak shift versus temperature.

Figure 5. Calculated values of diffusion energy for electrons (•) and holes (▪) versus temperature.

Figure 6. (a) Calculated values of σ versus temperature, (b) occupation factor for electrons (•) and holes (▪) versus excitation power density.
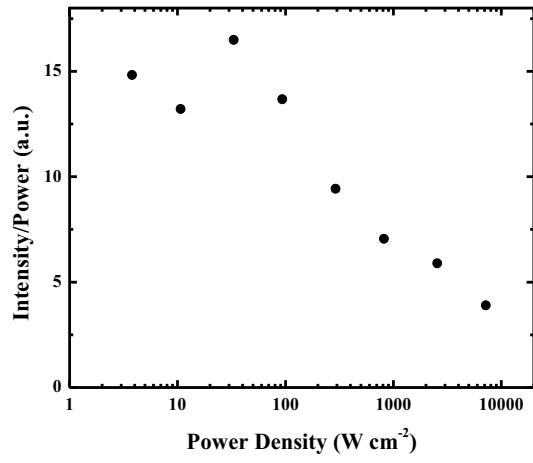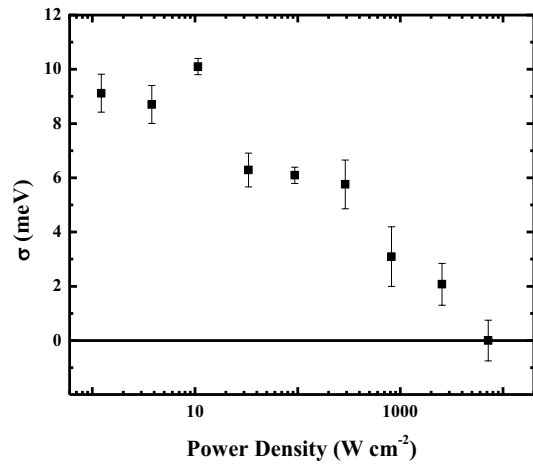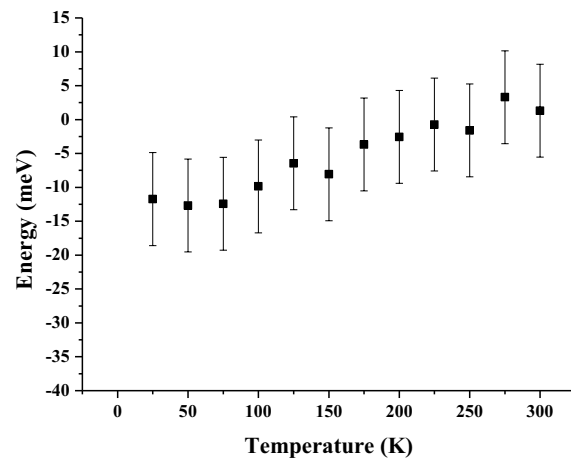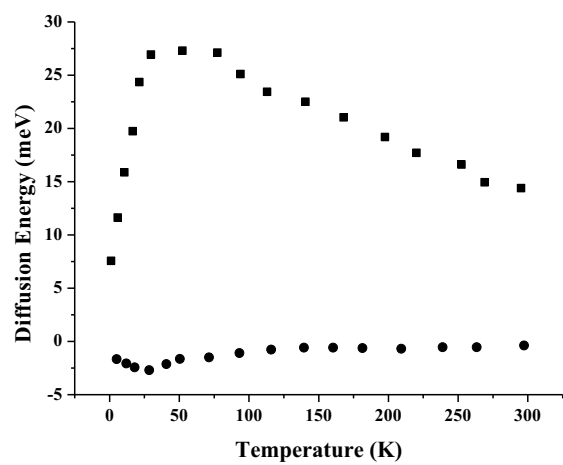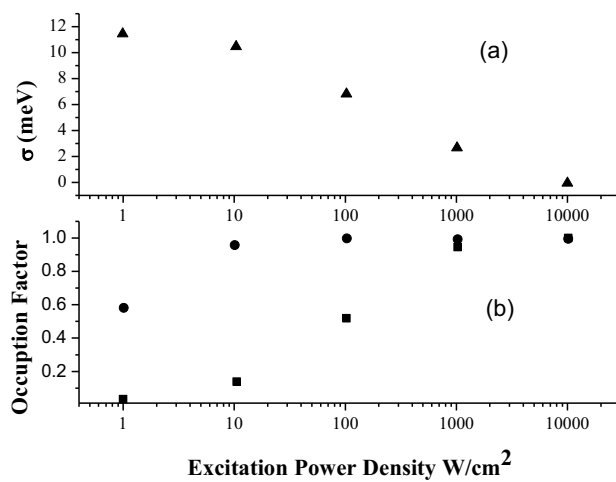
Figure 1
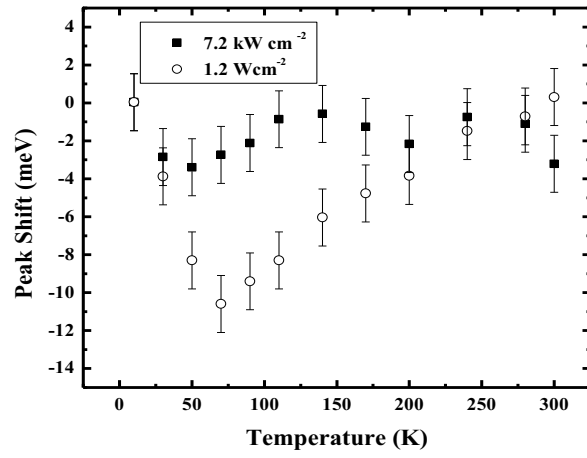
Figure 2

Figure 3

Figure 4

Figure 5

Figure 6